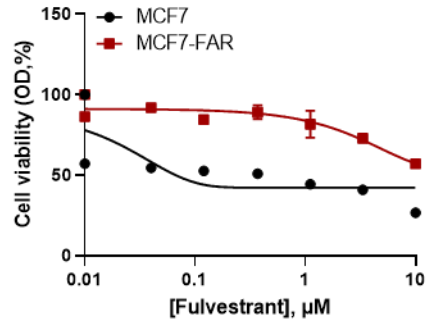
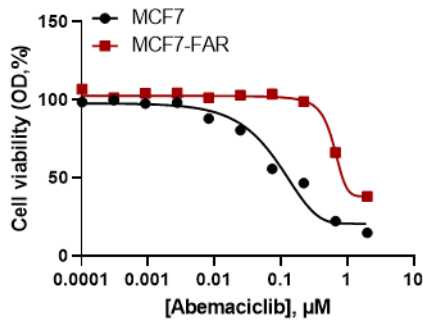
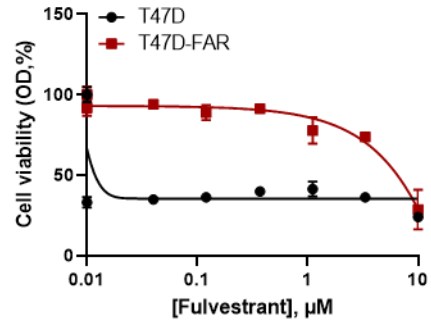
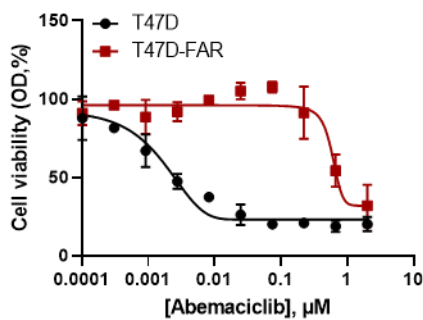


Supplementary Figure 1. Sensitivity of MCF-7-FAR and T47D-FAR cells to single drugs

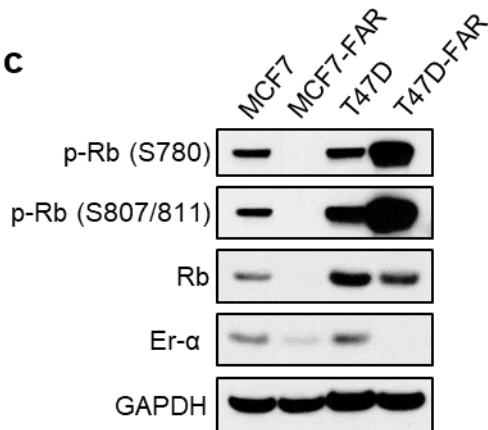
a



b

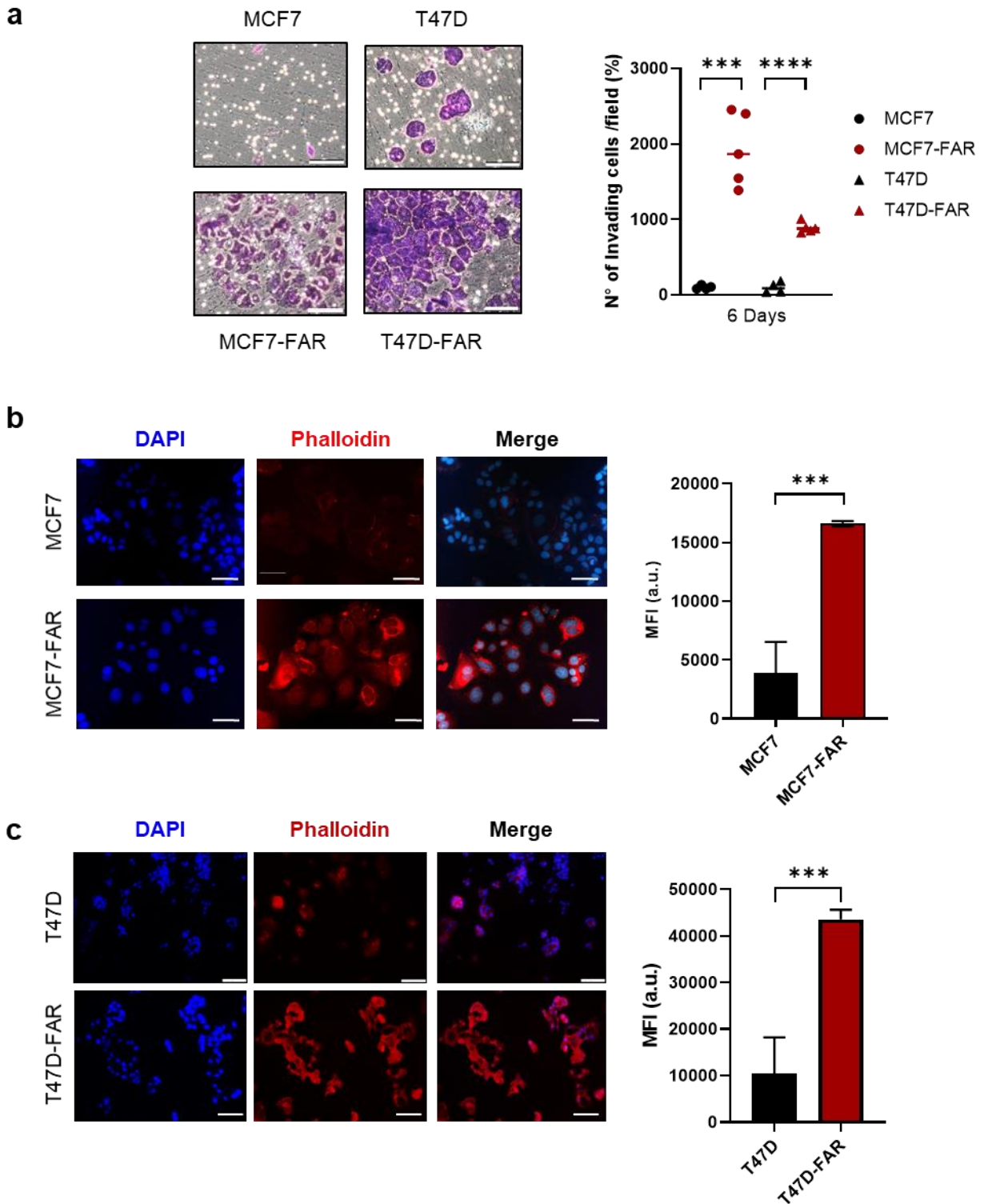


c



Supplementary Figure 1. Dose-response curves of MCF7, MCF7-FAR (**a**), T47D, T47D-FAR (**b**) exposed to increasing doses of fulvestrant or abemaciclib up to 10 μM or 2.5 μM concentrations, respectively, every 72 hours for 1 week, and then stained with crystal violet solution. Each data point represents the percent of cell viability relative to vehicle-treated controls, and shown as mean \pm SD from three independent experiments. Western blot for p-Rb (S780), p-Rb (S807/811), Rb, Er- α in MCF7, T47D parental and -FAR cells, treated with fulvestrant (1 μM) and abemaciclib (0.25 μM) for 18 hours. GAPDH was used as a loading control. Images are representatives from three independent experiments (**c**).

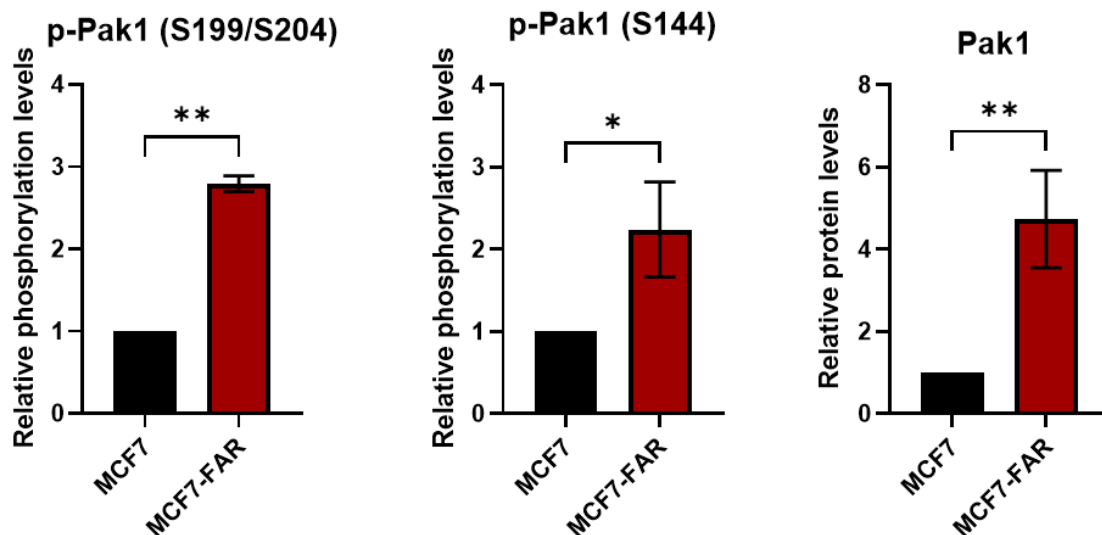
Supplementary Figure 2. Analysis of cytoskeleton rearrangement and migratory capability of FAR cells



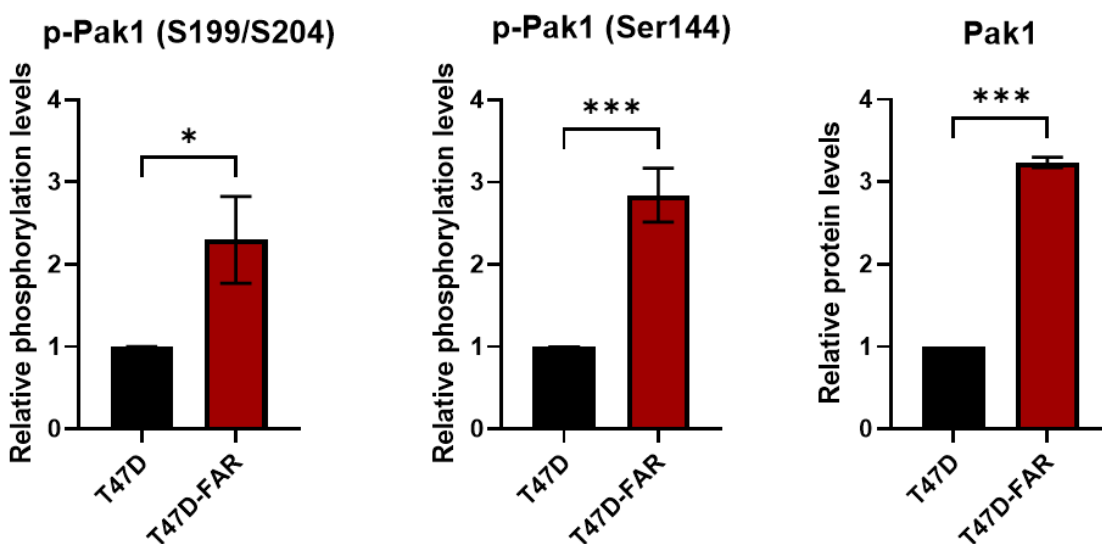
Supplementary Figure 2. Representative images of crystal violet stained MCF7, MCF7-FAR, T47D, or T47D-FAR invading cells through matrigel-coated transwell. All images were captured at 20x magnification (Bars = 200 μ m) (**a**). Scatter plot showing the mean of cell number *per* field reported as percentage relative to parental cells (**a, right**). Representative immunofluorescence (IF) staining for DAPI (blue) and Phalloidin (red) and merged images of MCF7 and MCF7-FAR cells (**b**) or T47D and T47D-FAR cells (**c**). All images were captured at 40x magnification (Bars = 50 μ m). Quantification of mean of fluorescence intensities was analyzed by ImageJ software. Data are plotted in the bar graphs as mean \pm SD of MCF7-FAR relative to MCF7 (**b, right**), and of T47D-FAR relative to T47D (**c, right**). For all panels, images are representatives from three independent experiments, performed in triplicates (** $p < 0.001$, **** $p < 0.0001$; *Student's T-test*).

Supplementary Figure 3. Analysis of protein expression levels of Pak1 in parental and FAR MCF7 or T47D.

a

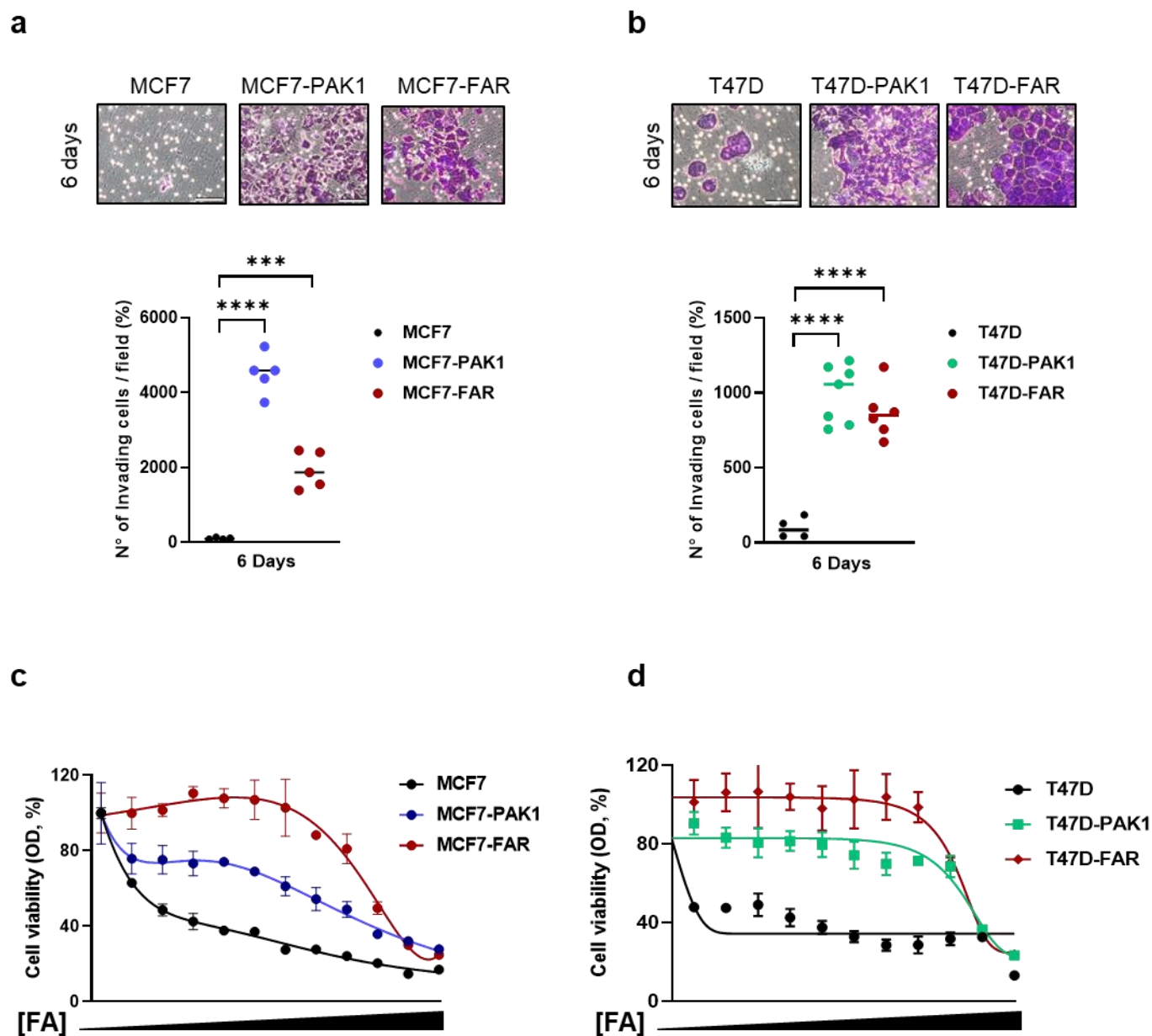


b



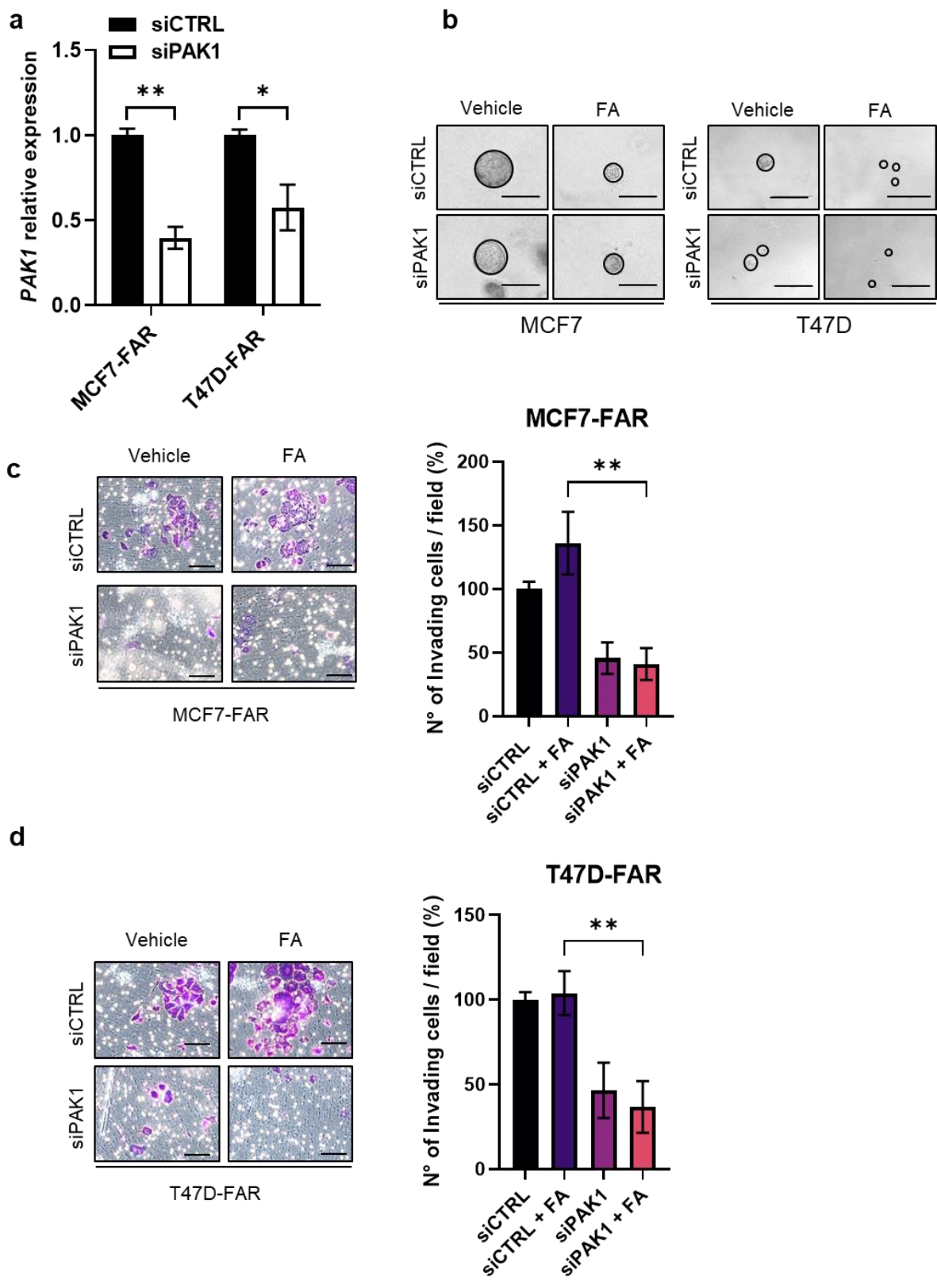
Supplementary Figure 3. Whole total lysates prepared from MCF7 and MCF7-FAR (a) or T47D, and T47D-FAR (b) were subjected to western blot analysis for p-Pak1 (S199/S204), p-Pak1 (S144); Pak1. Densitometric quantitation of the resulting molecular species performed using data from three independent experiments is reported in bar charts. Data are expressed as mean \pm standard deviation (* $p < 0,05$; ** $p < 0.01$, *** $p < 0.001$; Student's *T*-test).

Supplementary Figure 4: Invasive capability of *PAK1* over-expressing and FAR cells.



Supplementary Figure 4. Representative images of crystal violet stained MCF7, MCF7-PAK1, and MCF7-FAR (**a, top**) or T47D, T47D-PAK1, and T47D-FAR (**b, top**) invading cells through matrigel-coated transwell. All images were capture at 20x magnification (Bars = 200 μ m). Images are representative from three independent experiments, performed in triplicates. Scatter plot showing the mean of cell number *per* field reported as percentage relative to parental cells for MCF7 (**a, bottom**) and for T47D (**b, bottom**) models. Dose-response curves of MCF7, MCF7-PAK1, and MCF7-FAR (**c**) T47D, T47D-PAK1, and T47D-FAR (**d**) exposed to increasing doses of fulvestrant and abemaciclib (FA) up to 10 μ M or 2.5 μ M concentrations, respectively, every 72 hours for 1 week, and then stained with crystal violet solution. Each data point represents the percent of cell viability relative to vehicle-treated controls, and shown as mean \pm SD from two independent experiments. For all panels, (***) $p < 0.001$, (****) $p < 0.0001$; *Student's T-test*).

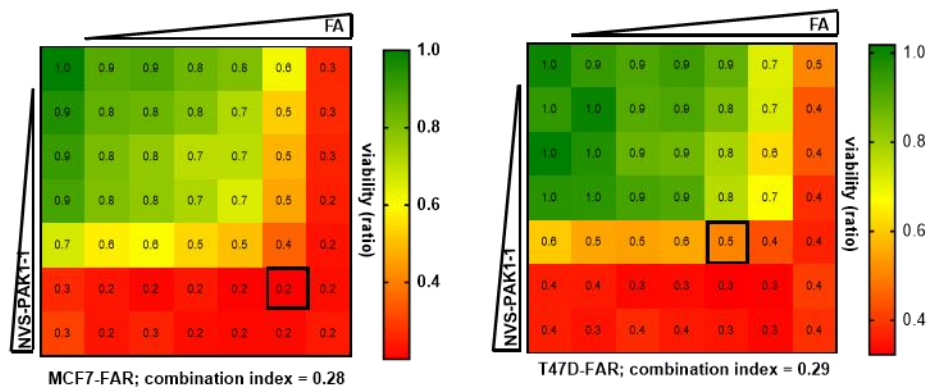
Supplementary Figure 5. PAK1 down-modulation impairs invasive capacity of MCF7-FAR and T47D-FAR cells



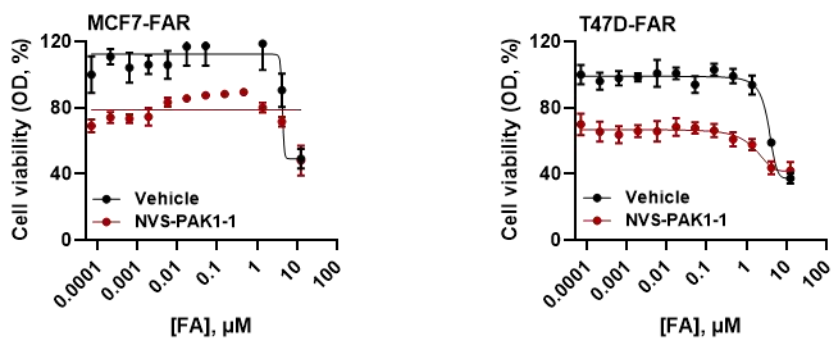
Supplementary Figure 5. Quantitative-PCR for *PAK1* gene expression 24 hours after siRNAs transfection in MCF7-FAR and T47D-FAR cells. Data are expressed as mean \pm SD relative to cells transfected with siRNA scrambled (siCTRL), from three independent experiments performed in triplicates ($*p < 0.05$; $**p < 0.01$, *Student's T-test*) (a). Representative images of spheroids embedded in collagen type I matrix set up from MCF7 (b, left) or T47D cells (b, right) transfected with 40 nM siRNA scrambled (siCTRL) or siRNA targeting *PAK1* (siPAK1) in presence of vehicle or 1 μ M fulvestrant and 0.25 μ M abemaciclib for 6 days. All images were capture at 20x magnification (Bars = 200 μ m). Images are representative from three independent experiments performed in triplicate. Representative images of crystal violet stained MCF7-FAR (c, left) or T47D-FAR (d, right) invading cells through matrigel-coated transwell, treated as described in panel b. Images are representative from three independent experiments, performed in triplicate. Bar graphs showing the mean of cell number *per field* reported as percentage relative to vehicle-treated controls for MCF7-FAR (c, right) and for T47D-FAR (d, right). For all panels, ($**p < 0.01$, *Student's T-test*).

Supplementary Figure 6. Impairment of FAR cell growth and invasion upon NVS-PAK1-1 treatment

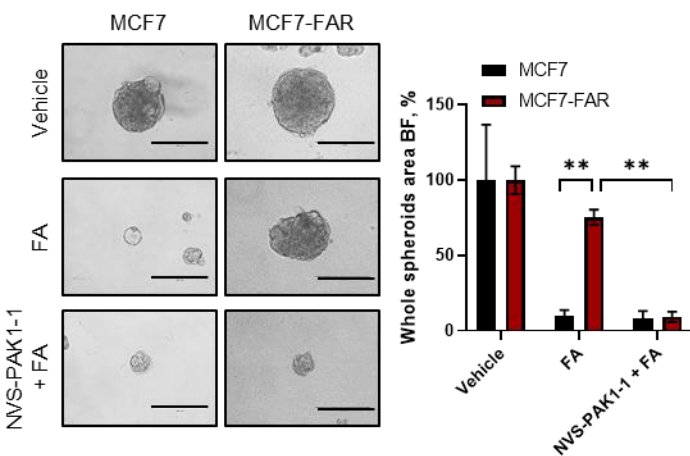
a



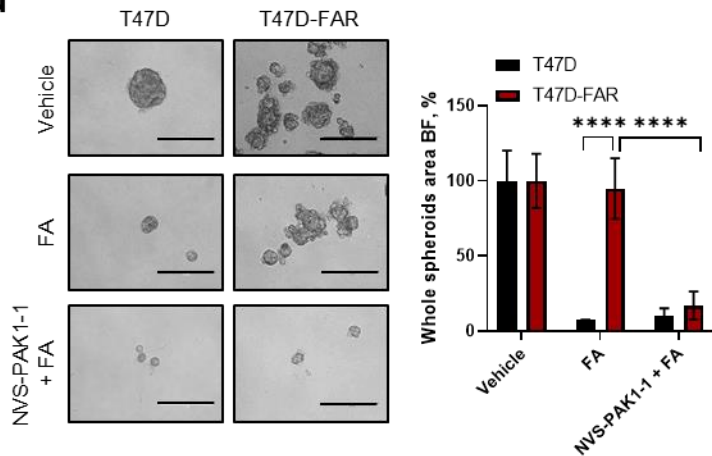
b



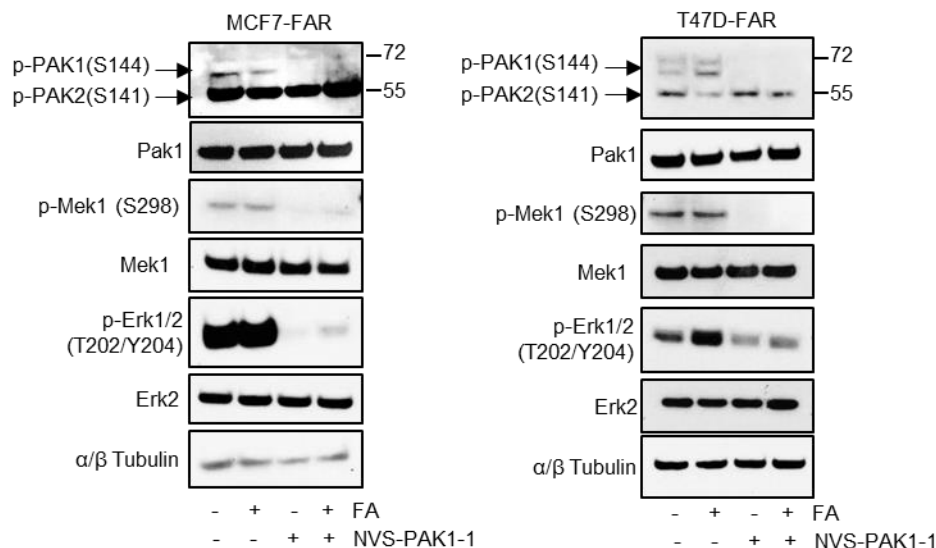
c



d

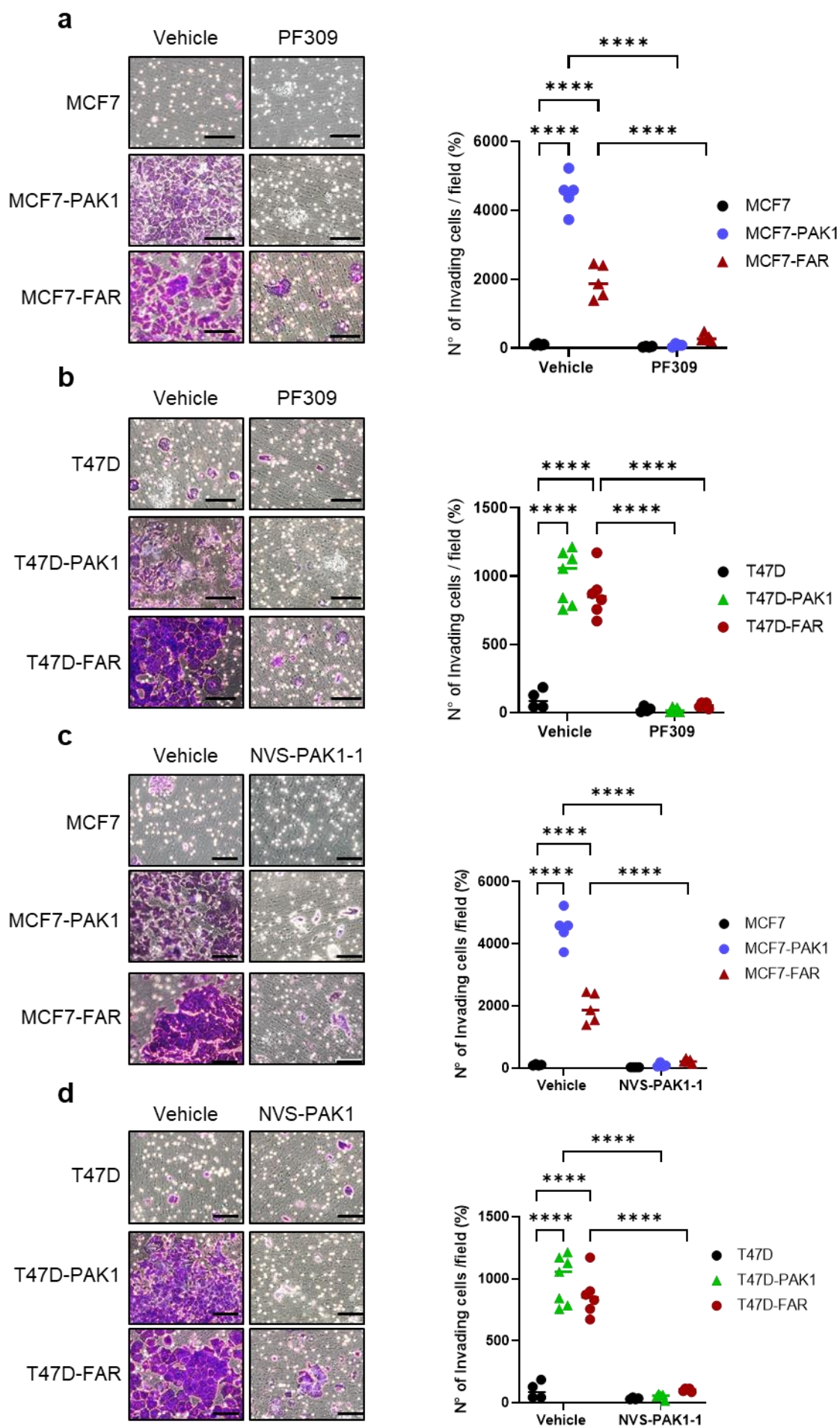


e



Supplementary Figure 6. Viability assays to test synergy between fulvestrant and abemaciclib (FA) and NVS-PAK1-1. Cells were treated with increasing concentrations of FA and NVS-PAK1-1 (up to 10 μ M and 100 μ M, respectively) alone or in combination every 72 h until vehicle-treated controls reached ~90% of confluence. Intensity values of cell monolayers stained with crystal violet were used to perform the Chou-Talalay test. Numbers inside each box indicate the *ratio* of viable treated cells to untreated cells from three independent experiments for MCF7-FAR (**a, left**) and for T47D-FAR (**a, right**). Dose-response curves of MCF7-FAR (**b, left**) or T47D-FAR (**b, right**) exposed to increasing doses of fulvestrant and abemaciclib (FA, up to 10 μ M fulvestrant and 2.5 μ M abemaciclib) in presence or not of 10 μ M NVS-PAK-1 for 1 week. Representative images of MCF7 and MCF7-FAR (**c, left**) or T47D and T47D-FAR (**d, left**) spheroids exposed to 400nM fulvestrant and 100nM abemaciclib (FA) \pm 5 μ M NVS-PAK1-1. Bar graphs showing percentage of whole spheroids area upon fulvestrant and abemaciclib (FA) \pm NVS-PAK1-1 treatment compared to spheroids treated with vehicle (plotted as 100%) are reported for MCF7 (**c, right**) and T47D (**d, right**) models. Western Blot analysis of MCF7-FAR (**e, left**) and T47D-FAR (**e, right**) treated with fulvestrant and abemaciclib (FA, 1 μ M and 0.25 μ M, respectively), NVS-PAK1-1 (40 μ M) or the combination for 48 hours. α/β tubulin was used as loading control. For all panels, data are plotted as means \pm SD of three independent experiments performed in triplicate or quadruplicate (** p < 0.01; **** p < 0.0001; 2way ANOVA Bonferroni's multiple comparisons).

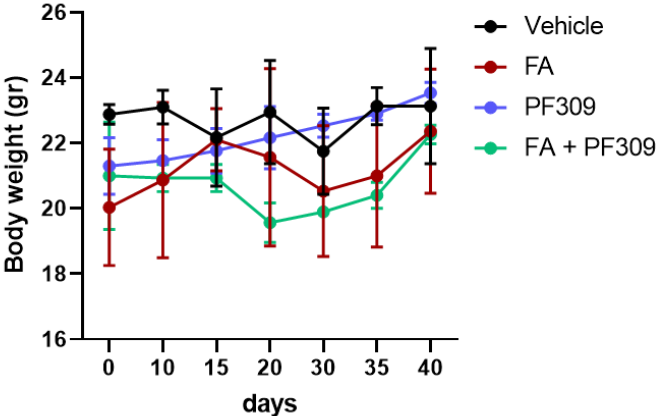
Supplementary Fig. 7: PF309 and NVS-PAK1-1 affect invasion of *PAK1* over-expressing and FAR cells



Supplementary Figure 7. Representative images of crystal violet stained MCF7, MCF7-PAK1, and MCF7-FAR invading cells, through matrigel-coated transwell, treated with 10nM PF309 (**a, left**) or NVS-PAK1-1 10 μ M (**c, left**) and T47D, T47D-PAK1 and T47D-FAR cells treated with 10nM PF309 (**b, left**) or NVS-PAK1-1 10 μ M (**d, left**) for 6 days. All images were captured at 20x magnification (Bars = 200 μ m). Images are representative from three independent experiments, performed in triplicates. Scatter plots showing the mean of cell number *per* field reported as percentage relative to parental cells MCF7 or T47D (**a-d, right**). Middle lines represent median. For all panels (** p <0.001, **** p <0.0001; 2way ANOVA Bonferroni's multiple comparisons).

Supplementary Figure 8. Body weight of Balb/c female

a



Supplementary Figure 8. Line chart showing body weight trend of Balb/c nude mice treated with vehicle, fulvestrant and abemaciclib (FA), PF309 and their combination as described in Fig.6 (a).

Figure 2

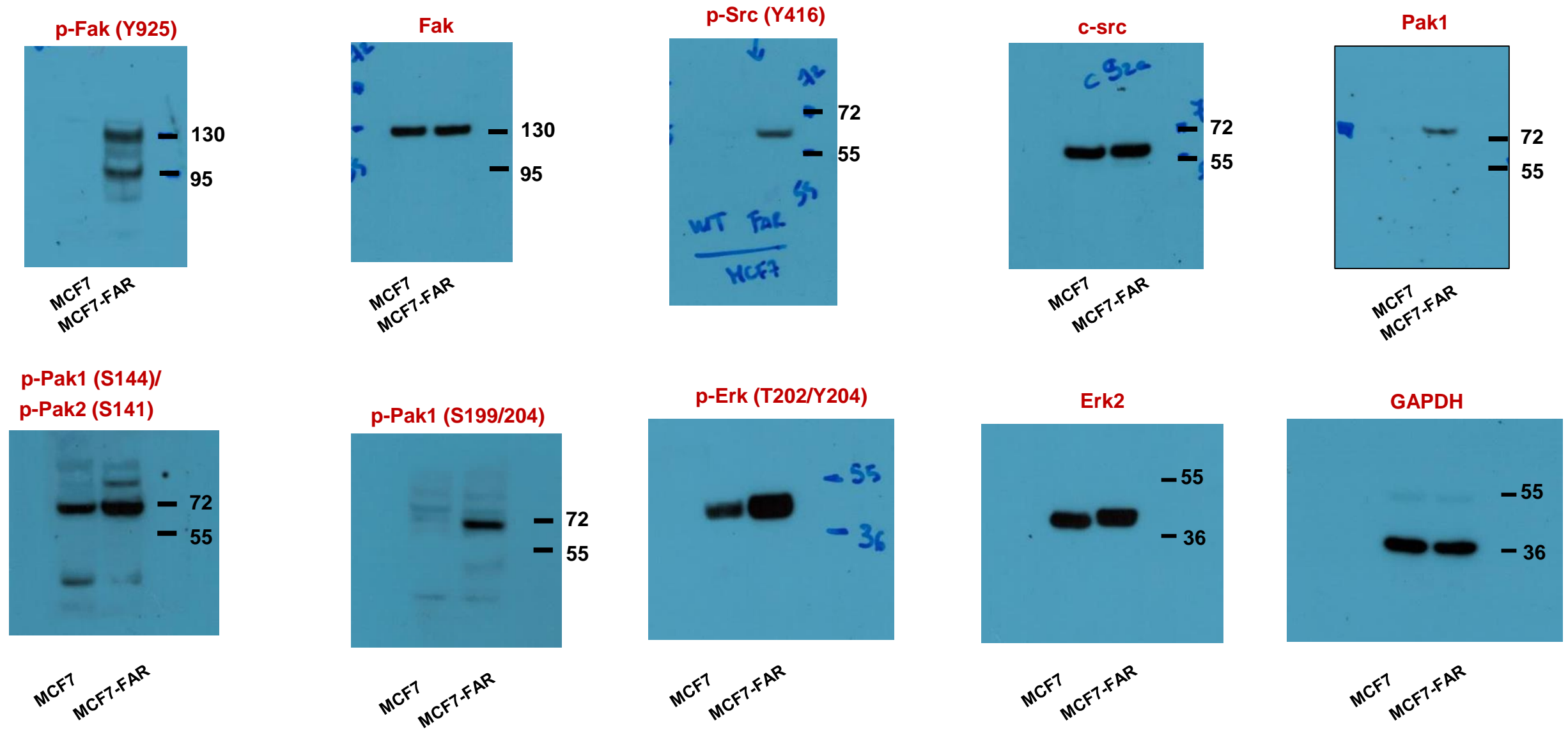


Figure 2

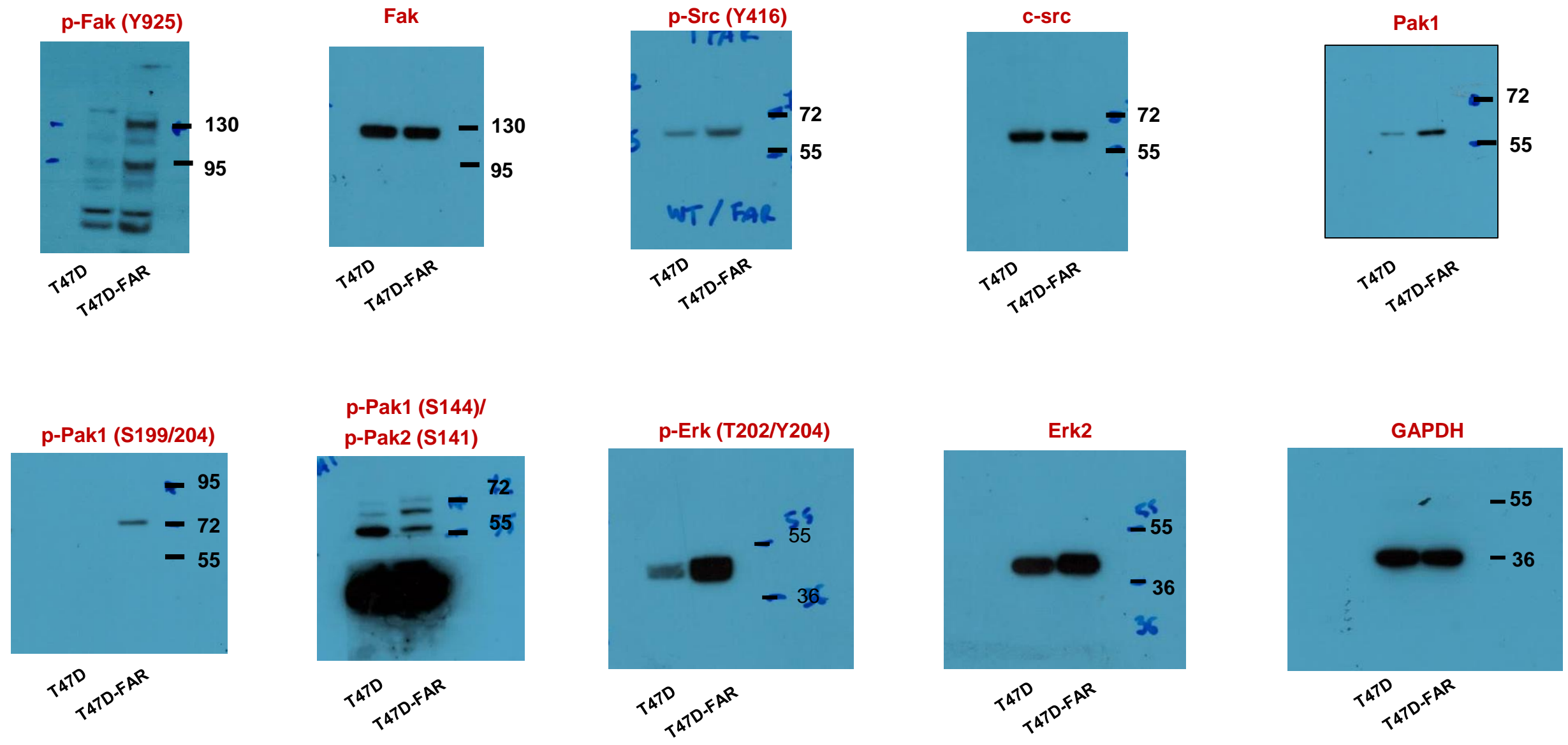


Figure 3

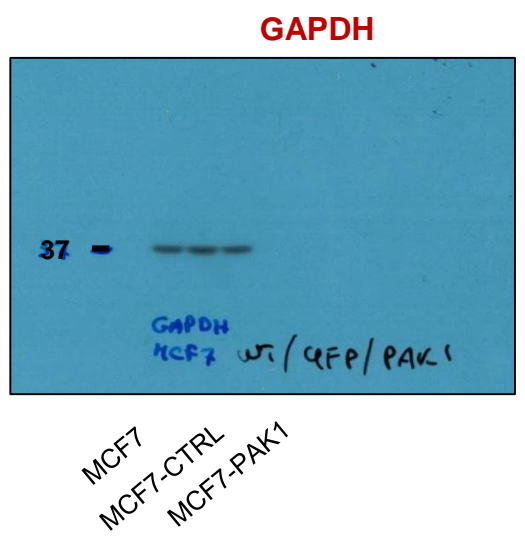
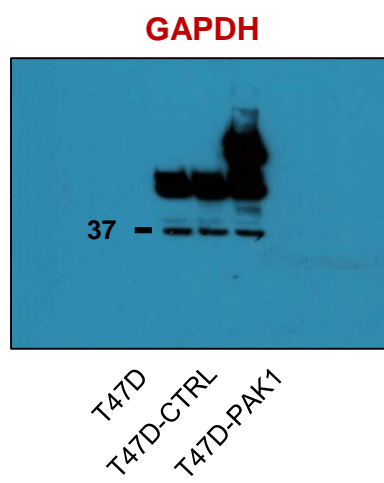
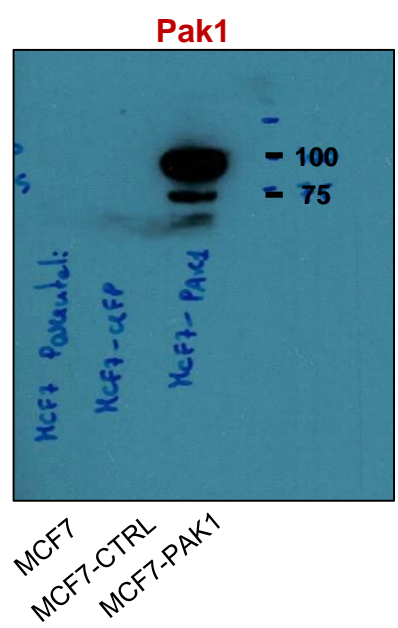
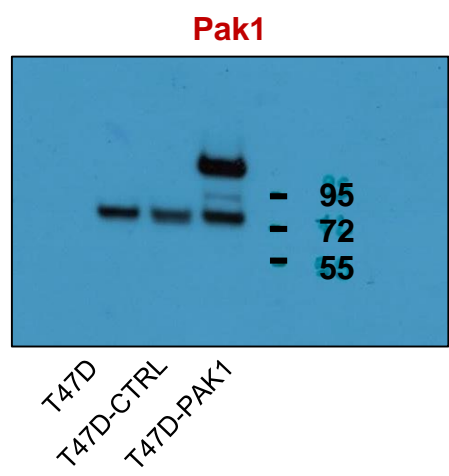


Figure 4

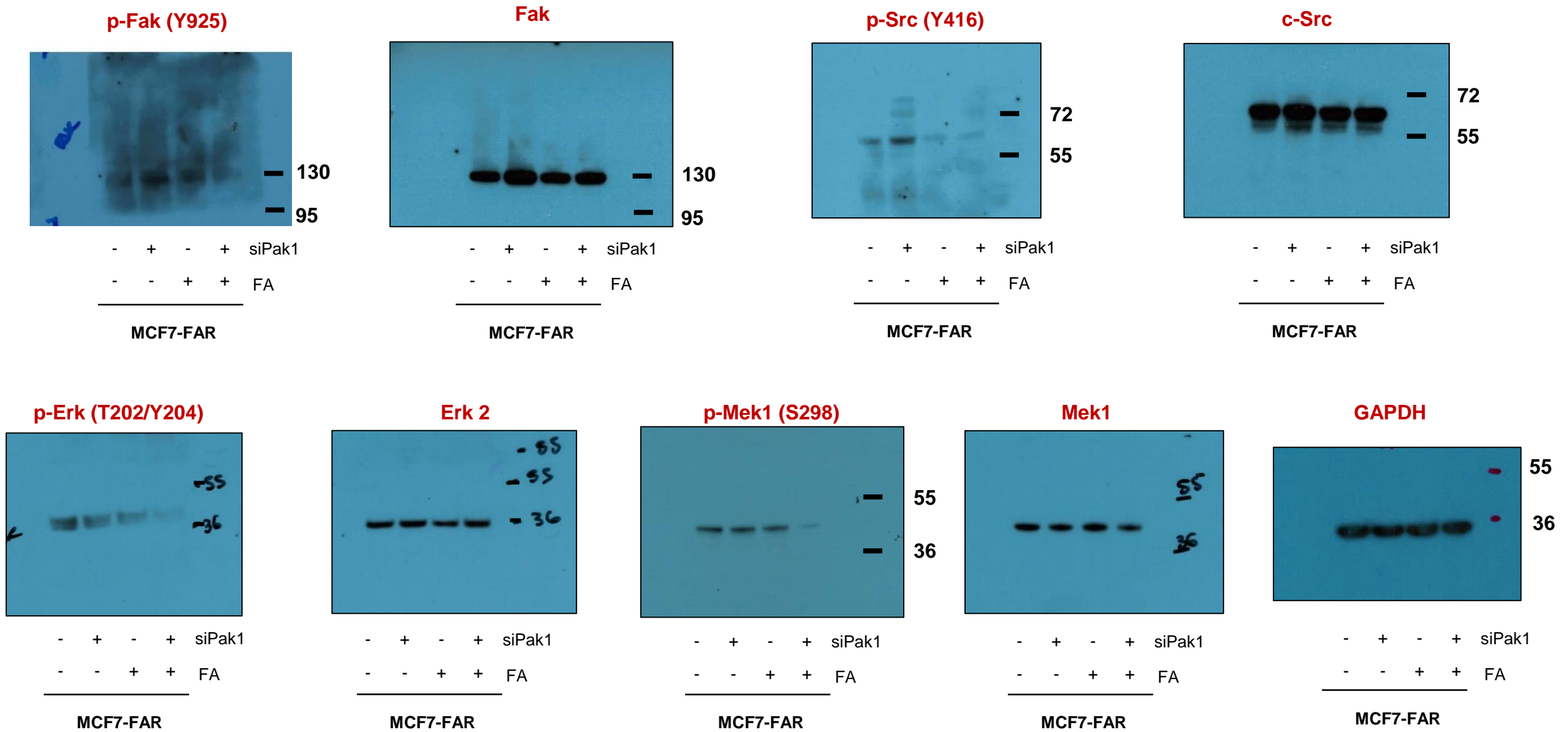
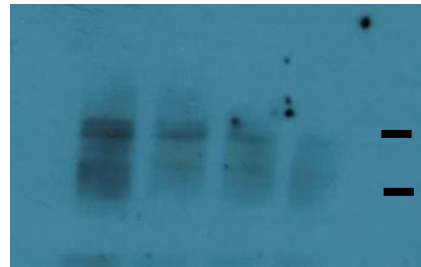


Figure 4

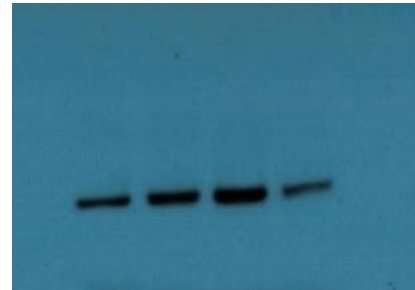
p-Fak (Y925)



- + - + siPak1
- - + + FA

T47D-FAR

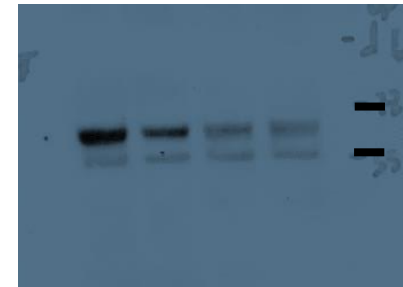
Fak



- + - + siPak1
- - + + FA

T47D-FAR

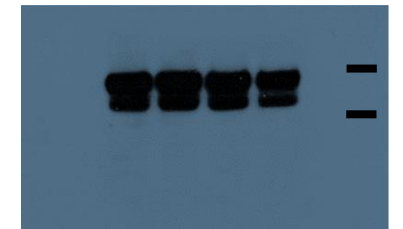
p-Src (Y416)



- + - + siPak1
- - + + FA

T47D-FAR

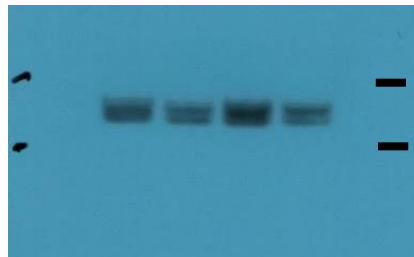
c-Src



- + - + siPak1
- - + + FA

T47D-FAR

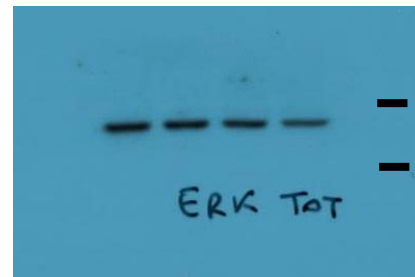
p-Erk (T202/Y204)



- + - + siPak1
- - + + FA

T47D-FAR

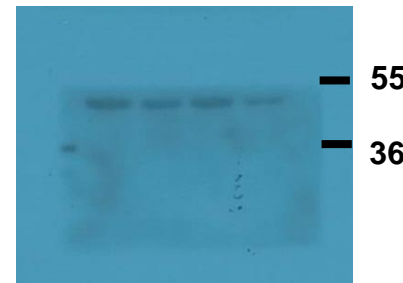
Erk2



- + - + siPak1
- - + + FA

T47D-FAR

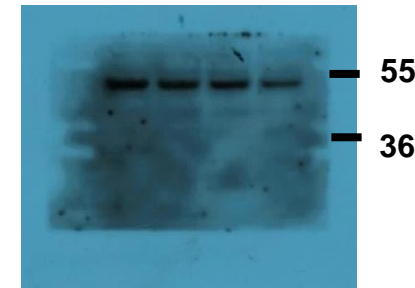
p-Mek1 (S298)



- + - + siPak1
- - + + FA

T47D-FAR

Mek1



- + - + siPak1
- - + + FA

T47D-FAR

GAPDH



- + - + siPak1
- - + + FA

T47D-FAR

Figure 5

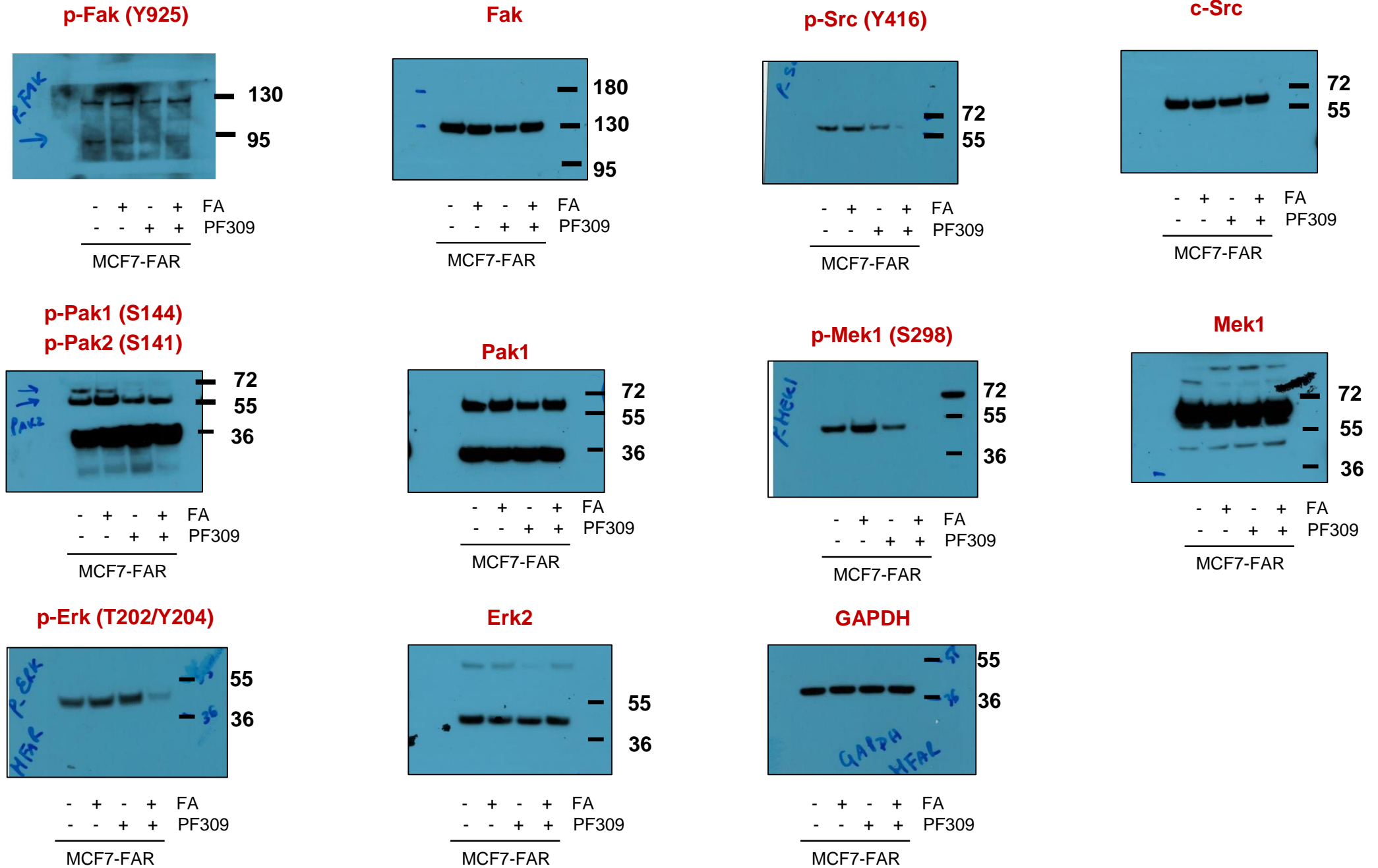


Figure 5

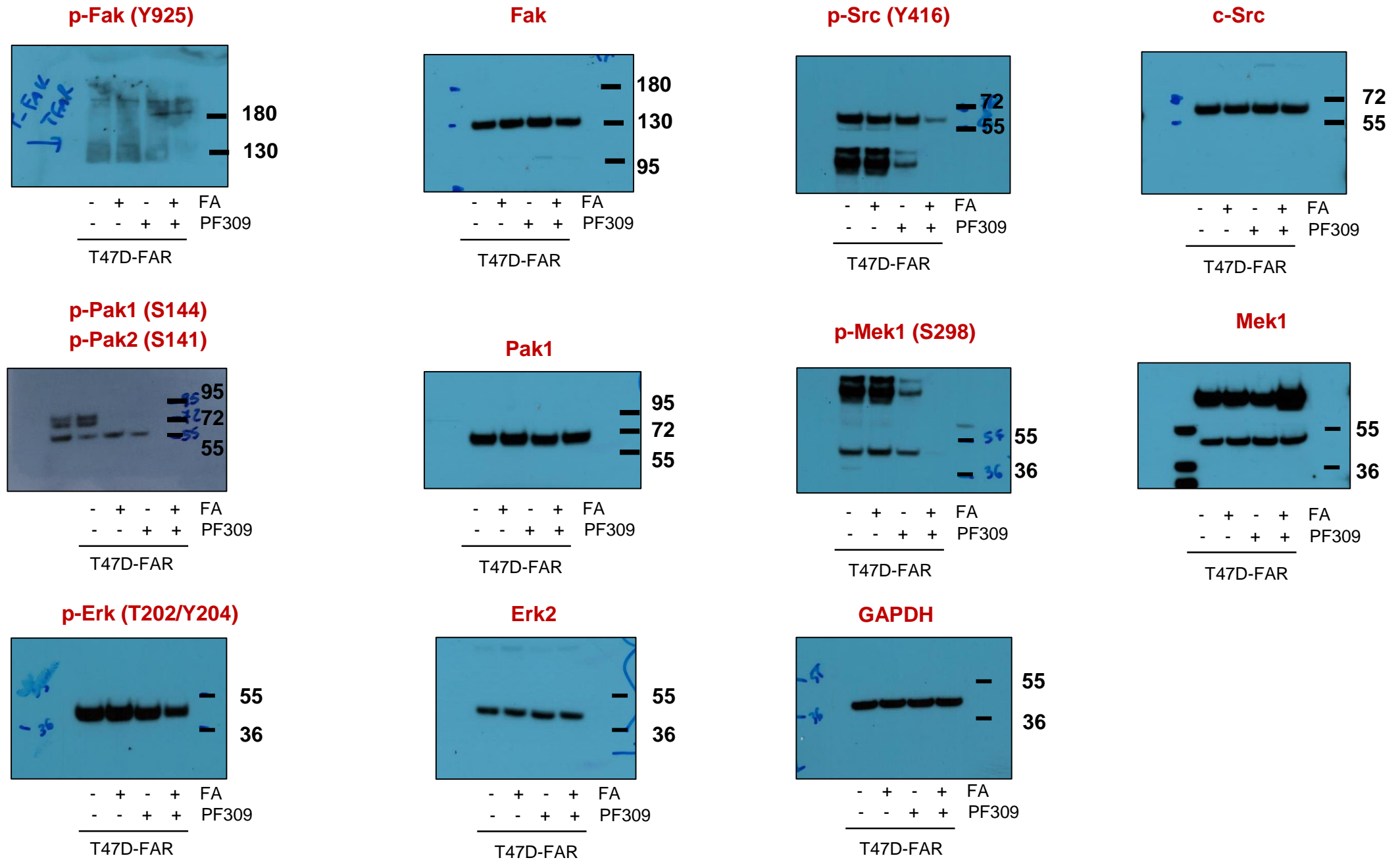
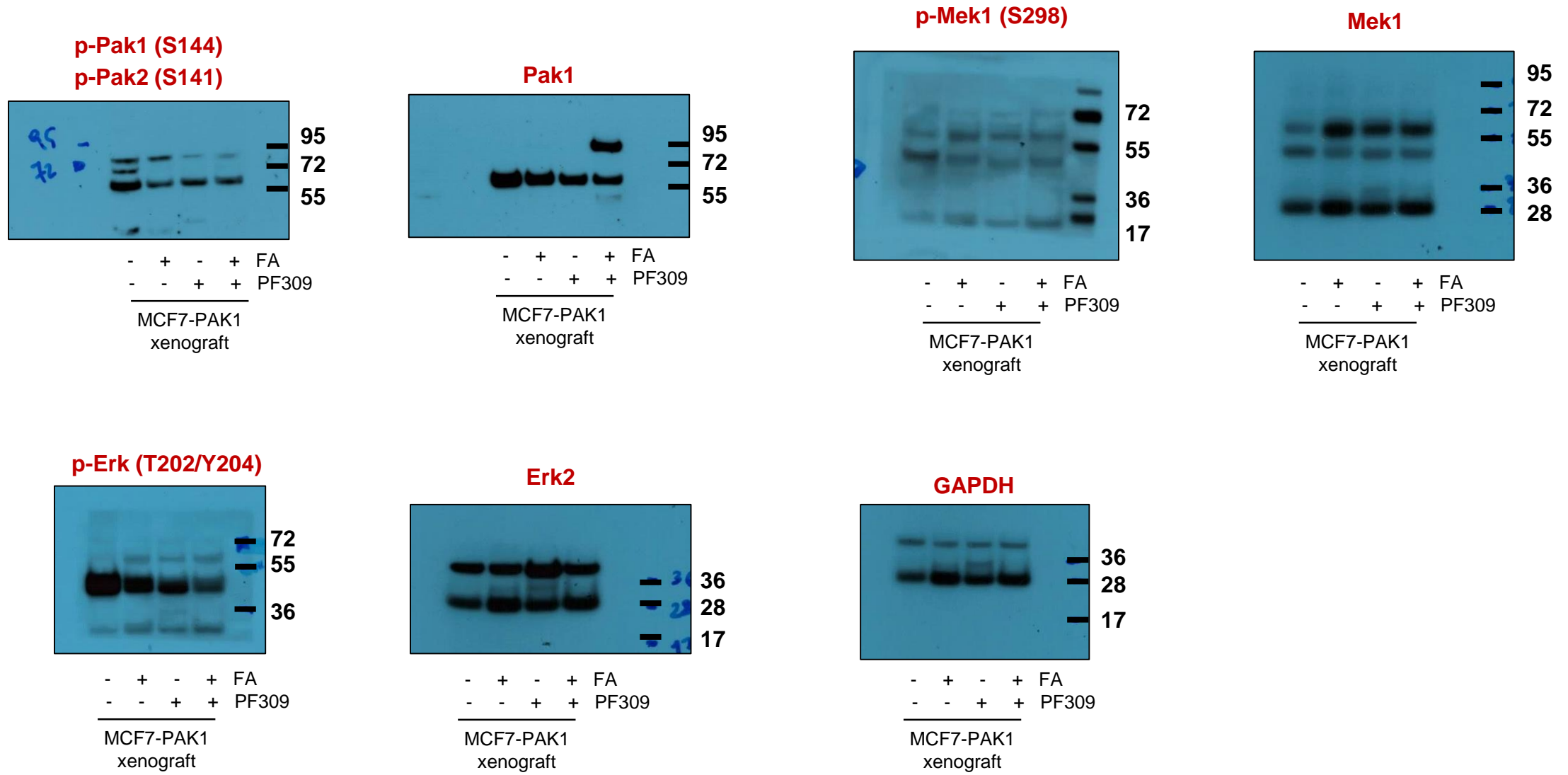
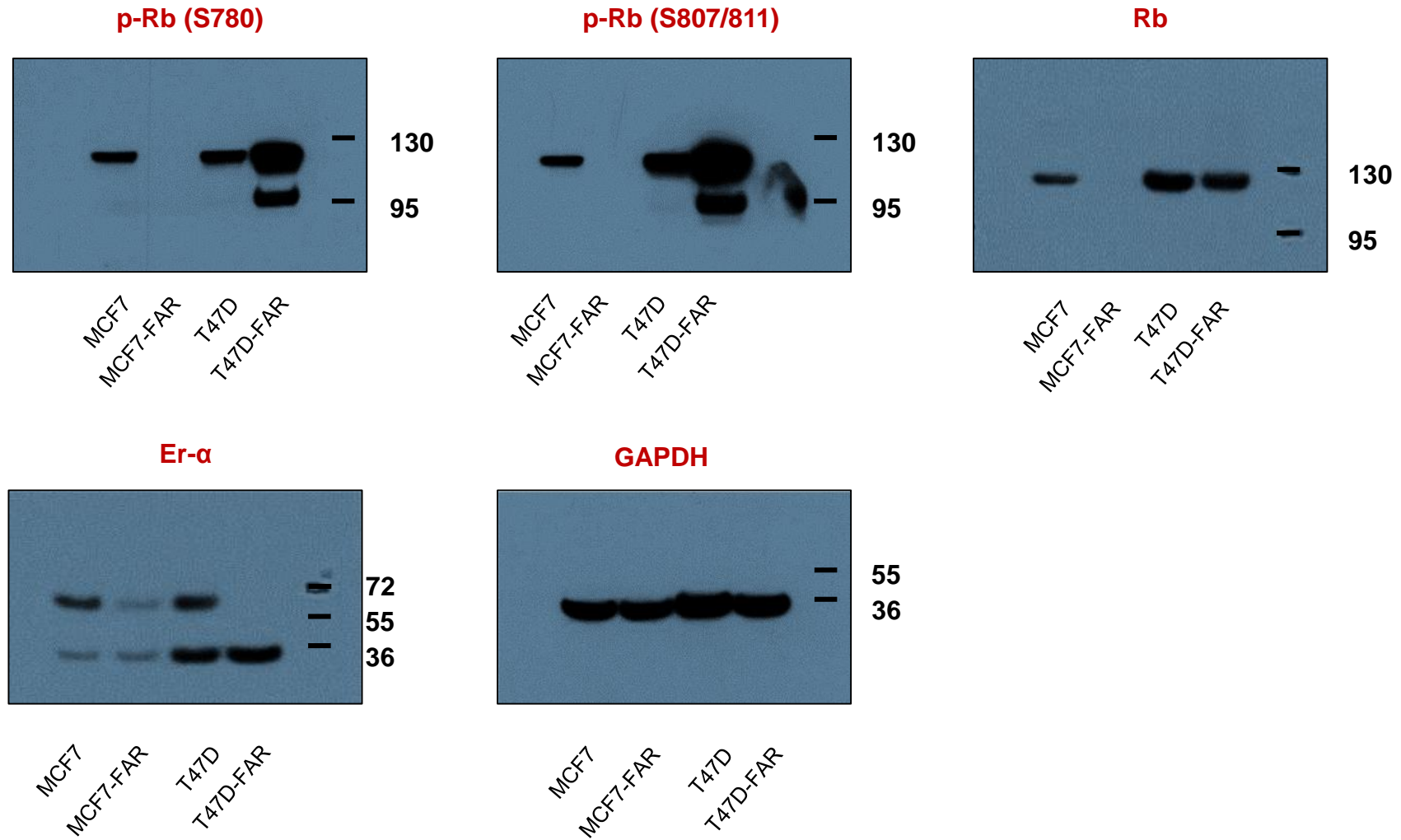


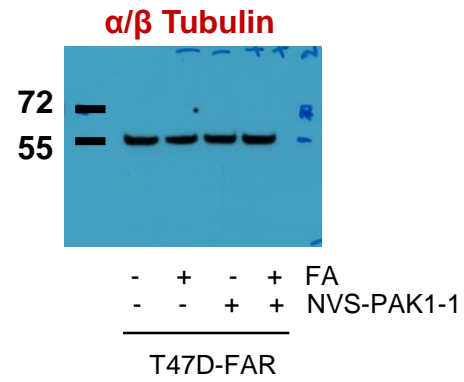
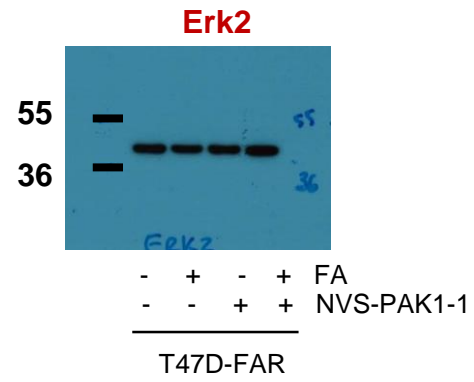
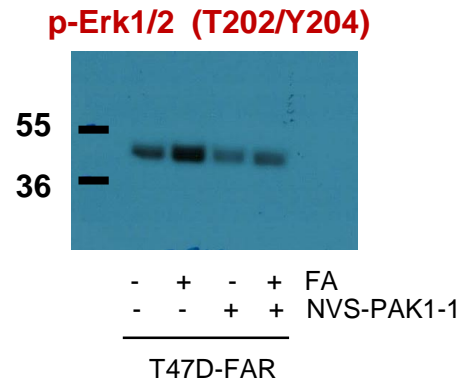
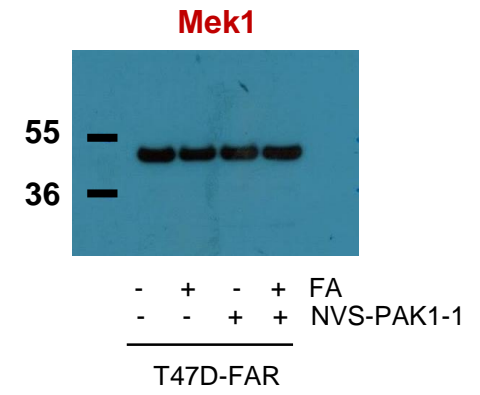
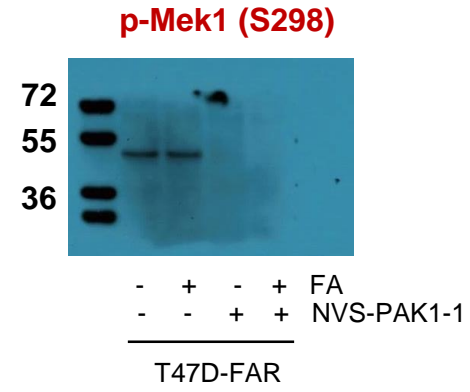
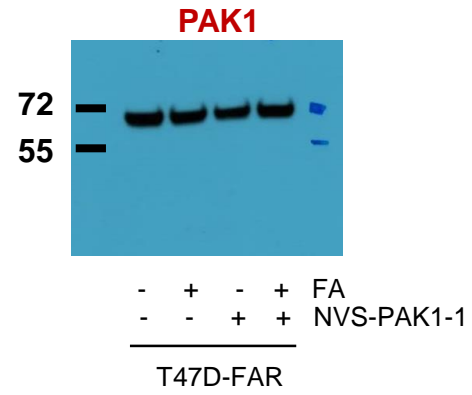
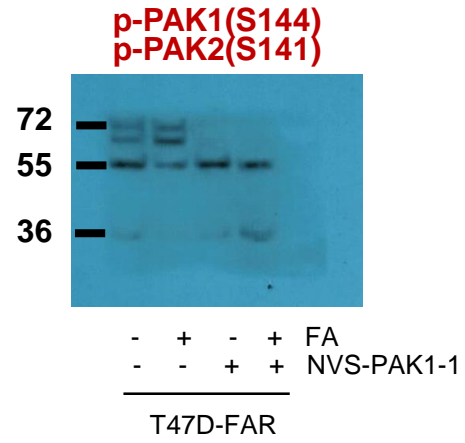
Figure 6



Supplementary Figure 1



Supplementary Figure 6



Supplementary Figure 6

